AFDEX Newsletter
Q2 / 2024
Adviser for metal Forming process Design EXpert

MFRC
Metal Forming Research Corporation
www.afdex.com, mfrc@afdex.com
Tel: +82-55-755-7529, Fax: +82-55-761-7529

Contents

1. AFDEX_V24R01 release

The V24R01 version will be released at the end of July 2024. New and improved features in AFDEX can be found in Sections 2 and 3.

2. New Features of AFDEX_V24R01

2.1. UI Changes

In V24R01, the pre-processor icon will be improved considering the characteristics of analysis input. You can check the changed pre-processor icons in Figure 2.1.

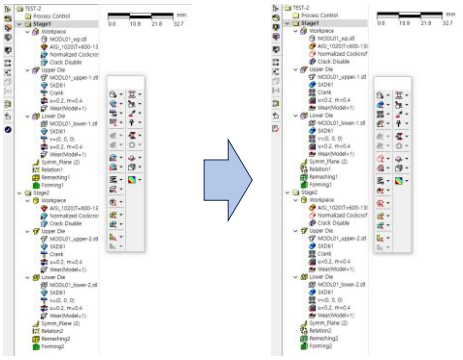

Figure 2.1 Improved preprocessor icon

2.2 View Function of Stress Triaxiality

In V24R01, a viewing function for stress triaxiality, that is, the mean stress divided by the strength, will be provided. It can be checked in the stress tab of the post-processor as shown in Figure 2.2.

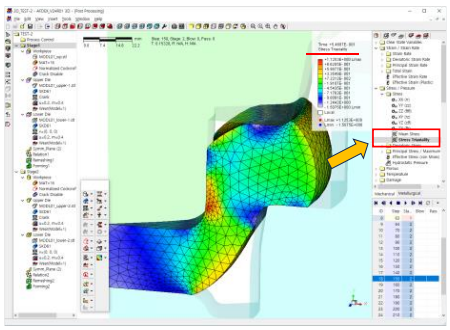

Figure 2.2 Stress triaxiality function

2.3 User Memo

V24R01 provides a new function that allows you to write detailed notes about the analysis information. To eliminate the inconvenience of writing a description in a file name or folder name, a description field was added to the AFDEX project file. Multilingual input is possible, including Korean, English, Japanese, etc.

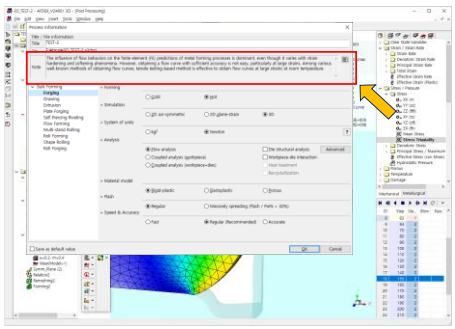

Figure 2.3 Entering user description

3. Improvements of AFDEX_V24R01

3.1 Typical Flow Curve and Tensile Testing at Room Temperature

Strain hardening capability has a significant impact on cold plastic deformation. For example, obtaining wrinkled prediction results as shown in the experiment in Figure 3.1, accurate flow curves, that is, accuracy of strain hardening capability, which must be supported along with high-performance mesh regeneration techniques. Please refer to the following paper regarding the effect of strain hardening on plastic deformation. [Eom, J. G. et al., 2014, Effect of strain hardening capability on plastic deformation behaviors of material during metal forming, Mater. Des.]

(a) Experimental

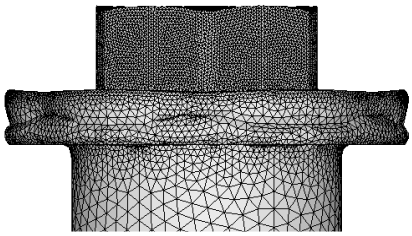

(b) Predictions

Figure 3.1 Prediction of wrinkles generated during bolt head forming (MFCAE 2014, SFJ, Jinju)

However, it is not easy to practically obtain strain hardening capability for the large strain required in forging simulation. Therefore, it is believed that most of the flow curves at large strains in the literature were assumed. When analyzing the tensile test using the flow function, it is easy to see that this assumed flow curve is significantly different from reality.

The following paper presents a practical method of obtaining flow stress at large strains using tensile testing. [Joun, M. S. et al., 2008, A new method for acquiring true stress-strain curves over a large range of strains using a tensile test and finite element method, Mech. Mater.] Based on this method, AFDEX /MAT was developed, and this program made it possible to calculate a flow stress at large strain (1.6 for SCM435). As a result, high-accuracy analysis of tensile testing became possible, and thus unknown flow characteristics such as damage value at fracture point could be scientifically obtained. A variety of applications can be found in several applied papers. Here, we introduce four representative flow curves.

Summarizing the results of many years of research on flow curves at room temperature conducted by the AFDEX developer group, flow characteristics can be divided into four basic strain hardening capabilities (Figure 3.2). In the figure, the lower part shows the predicted results of the tensile testing, and the upper part shows the corresponding flow curve. As can be seen from the related literature, the predicted tensile testing curve accurately represents the experiments.

Most of general carbon steel and alloy steels exhibit a typical monotonic strain hardening capability, as can be seen in a flow curve widely used for educational purposes shown in Figure 3.2(a). In this case, the flow curve may be expressed as a typical classical flow function, for example, mathematical models such as Hollomon, Ludwik, and Swift. Of course, from a tensile testing perspective, these traditional mathematical models have limitations in expressing the monotonic strain hardening. This is because traditional flow functions other than Voce cannot reflect the considerable decrease in strain hardening increment due to the increase in dislocation.

The strain hardening capability of steel or non-ferrous metals that have undergone a number of special heat treatments may not be monotonic. Figure 3.2(b) shows the tensile testing and flow curve of SUS304. It exhibits typical double strain hardening capability. The SUS304 is characterized by the necking occurring at a large engineering strain and the ratio of tensile strength to yield strength is large. Since this, it undergoes rapid strain hardening up to a strain of around 0.5, but the strain hardening is alleviated after the necking. Judging based on strain hardening of 0.5 or less, cold forming of SUS304 is impossible. However, cold forming is possible if the temperature softening phenomenon caused by heat generation and low strain hardening capability at large strains are considered.

Figure 3.2(c) shows the results of tensile testing and flow curve of A6061-T6 alloy, showing the perfectly-plastic strain hardening capability after high strain hardening at low strains.

Figure 3.2(d) is for ESW105, showing a particular tensile testing and flow curve where necking occurs from the beginning. ESW is pre-heat treated and aims to be eco-friendly and cost-saving by omitting post-forging heat treatment. ESW is characterized by the high-strength and strain softening due to the effect of pre-heat treatment but forging is possible because a certain degree of elongation is guaranteed despite no strain hardening.

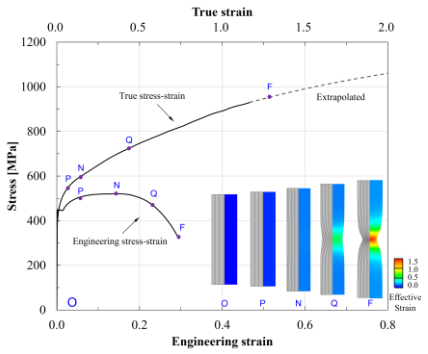

(a) Forging increased strain hardening

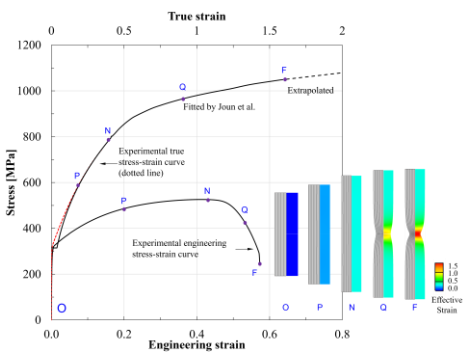

(b) Double curvature strain hardening

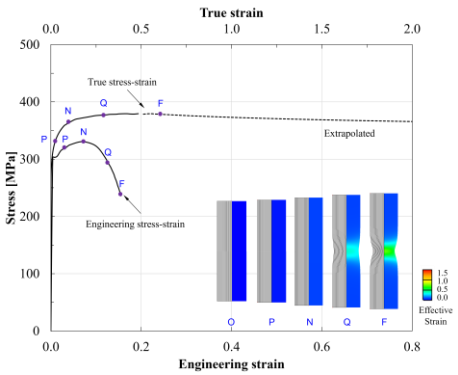

(c) Fully plastic after low strain rate strain hardening

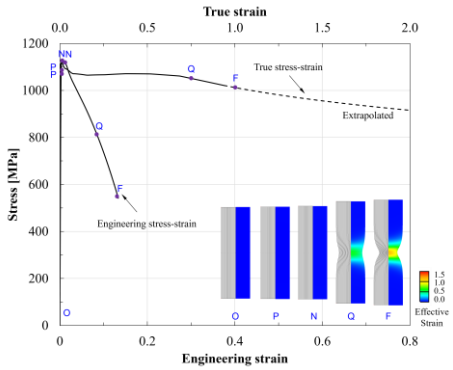

(d) Low strain rate Deformation softening after complete plasticity

Figure 3.2 Four representative tensile testing and flow curves

Meanwhile, Figure 3.3 shows the FE-predicted deformed shapes of the tensile test specimen at the point of fracture obtained as the FE predictions of tensile test of the four materials mentioned above. Although the sizes of the specimens used in Figure 3.2 are different from each other, notably, the same standard specimen was used to obtain the analysis results of Fig. 3.3 for the sake of comparison.

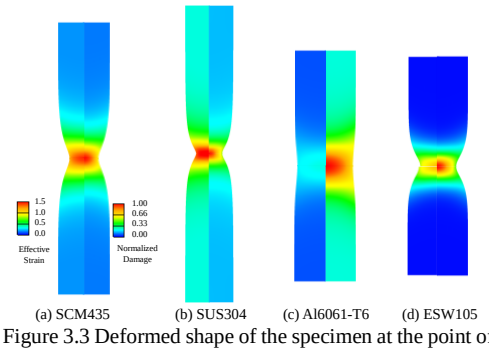

(a) SCM435 (b) SUS304 (c) Al6061-T6 (d) ESW105

Figure 3.3 Deformed shape of the specimen at the point of fracture predicted using the same standard specimen

3.2 Binder Load Improvement

Previously, the load imposed on a binder should be given as a function of absolute time or distance. In V24R01, the binder load can be given as a function of a relative displacement between the binder and dies. Accordingly, the input window of the pre-processor is modified to allow to enter the relative displacement of the binder die to a reference die and the corresponding load information.

3.3 Velocity Components View Feature in Post-Processor

The previous version has provided the velocity field view feature for only XX, YY, ZZ, and total XYZ. In V24R01, it is improved to show the sum of two components of velocity at the request of users: XY, YZ, and ZX. This feature is available in the Nodal Velocity tab submenu of the post-processor as shown in Figure 3.3.

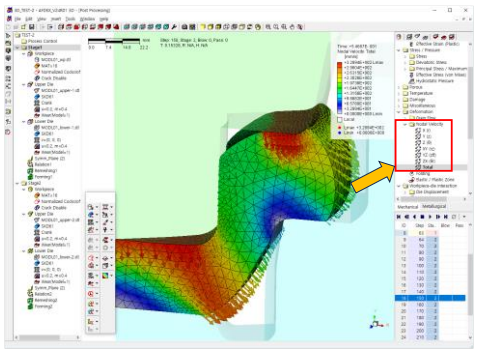

Figure 3.3 Velocity field view feature in AFDEX post-processor

3.4 Automatic Initialization of Die Position

Previously, when calculating an edge contact between objects, its accuracy varied depending on mesh system. In V24R01, the error of the automatic die position initialization function was much reduced by improving the calculation method for the edge contact between objects. Figure 3.4 shows the improvements of the automatic die position initialization feature.

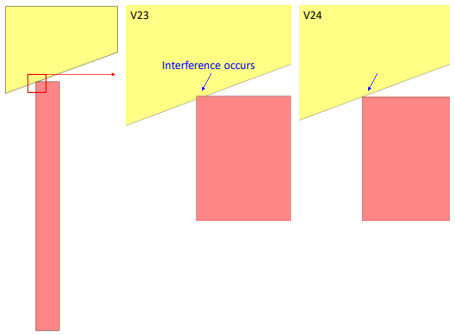

Figure 3.4 Automatic initialization of die position

3.5 User-Friendly Legend Range Settings in Post-Processer

Until the previous version, when multiple objects including the materials and dies are simulated at the same time, the range limits of the legend are determined by the minimum and maximum values of the simulation results (stress, strain, etc.) for all objects regardless of the objects selected for visualization purpose. In V24R01, the range limits of the legend are set by the minimum and maximum values of the analysis results for the objects selected for visualization, as shown in Figure 3.5. Non-selected objects have nothing to do with it.

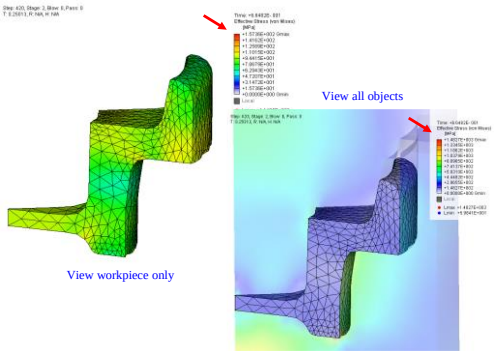

Figure 3.5 Automatic conversion of state variables

4. Notice

4.1 Online Learning in 2024

Education of the theory and usage through the YouTube channel has recently been significantly reorganized. You can check out the theory of engineering plasticity and finite element method and how to use AFDEX on the AFDEX's official YouTube channel. In addition, lectures on statics, solid mechanics, and mathematics are provided for non-majors.

AFDEX's official YouTube address is as follows. (https://www.youtube.com/c/AFDEX)

4.2 9th JSTP ISPF International Seminar on Precision Forging

9th JSTP (The Japan Society for Technology of Plasticity) ISPF International Seminar on Precision Forging was held for 5 days from March 11th to March 15th at Kyoto, Japan. This event included a seminar, oral/poster presentations, group project and plant tour. MFRC presented a webinar entitled, "Numerical Study of Temperature and Strain Rate Sensitivity on Recrystallization of Cogging Process of M50 Bearing Steel."